

# Kinetic effects of temperature on rates of genetic divergence and speciation

Andrew P. Allen\*<sup>†</sup>, James F. Gillooly<sup>‡</sup>, Van M. Savage<sup>§</sup>, and James H. Brown\*<sup>¶</sup>

\*National Center for Ecological Analysis and Synthesis, 735 State Street, Suite 300, Santa Barbara, CA 93101; <sup>‡</sup>Department of Zoology, University of Florida, Gainesville, FL 32611; <sup>§</sup>Bauer Center for Genomics Research, Harvard University, Boston, MA 02138; and <sup>¶</sup>Department of Biology, University of New Mexico, Albuquerque, NM 87131

Contributed by James H. Brown, May 2, 2006

Latitudinal gradients of biodiversity and macroevolutionary dynamics are prominent yet poorly understood. We derive a model that quantifies the role of kinetic energy in generating biodiversity. The model predicts that rates of genetic divergence and speciation are both governed by metabolic rate and therefore show the same exponential temperature dependence (activation energy of  $\approx 0.65$  eV;  $1 \text{ eV} = 1.602 \times 10^{-19}$  J). Predictions are supported by global datasets from planktonic foraminifera for rates of DNA evolution and speciation spanning 30 million years. As predicted by the model, rates of speciation increase toward the tropics even after controlling for the greater ocean coverage at tropical latitudes. Our model and results indicate that individual metabolic rate is a primary determinant of evolutionary rates:  $\approx 10^{13}$  J of energy flux per gram of tissue generates one substitution per nucleotide in the nuclear genome, and  $\approx 10^{23}$  J of energy flux per population generates a new species of foraminifera.

allopatric speciation | biodiversity | macroevolution | metabolic theory of ecology | molecular clock

The latitudinal increase in biodiversity from the poles to the equator is the most pervasive feature of biogeography. For two centuries, since the time of von Humboldt, Darwin, and Wallace, scientists have proposed hypotheses to explain this pattern. New species arise through the evolution of genetic differences among populations from a common ancestral lineage (1–4). Many hypotheses therefore attribute the latitudinal biodiversity gradient to a gradient in speciation rates caused by some independent variable, such as earth surface area or solar energy input (5–7). Some fossil data suggest that speciation rates do indeed increase toward the tropics (8–10), but these findings remain open to debate due in part to our limited understanding of the factors that control macroevolutionary dynamics.

Recent advances toward a metabolic theory of ecology (11) provide new opportunities for assessing the factors that control speciation rates. This recent work indicates that two fundamental variables influencing the tempo of evolution, the generation time, and the mutation rate (3) are both direct consequences of biological metabolism (12–14). Here we combine these recent insights from metabolic theory with the theory of population genetics to derive a model that predicts how environmental temperature, through its effects on individual metabolic rates (Eqs. 1–4), influences rates of genetic divergence among populations (Eqs. 5–7) and rates of speciation in communities (Eqs. 8 and 9). We evaluate the model by using data from planktonic foraminifera, because this group has extensive DNA sequence data for evaluating population-level predictions on genetic divergence combined with an exceptionally complete fossil record for evaluating community-level predictions on speciation rates.

## Model Development

The two individual-level variables constraining the evolutionary rate of a population, the generation time, and the mutation rate (3) are both direct consequences of biological metabolism (15, 16). They are both governed by the body size- and temperature-

dependence of mass-specific metabolic rate,  $\bar{B}$  ( $\text{J}\cdot\text{sec}^{-1}\cdot\text{g}^{-1}$ ) (12–14):

$$\bar{B} = B/M = b_o M^{-1/4} e^{-E/kT} = B_o e^{-E/kT}, \quad [1]$$

where  $B$  is individual metabolic rate ( $\text{J}\cdot\text{sec}^{-1}$ ),  $M$  is body mass ( $\text{g}$ ),  $T$  is absolute temperature ( $\text{K}$ ),  $B_o$  is a normalization parameter independent of temperature ( $\text{J}\cdot\text{sec}^{-1}\cdot\text{g}^{-1}$ ) that varies with body size as  $B_o = b_o M^{-1/4}$  (12), and  $b_o$  is a normalization parameter independent of body size and temperature that varies among taxonomic and functional groups (12, 17). The Boltzmann–Arrhenius factor,  $e^{-E/kT}$ , characterizes the exponential effect of temperature on metabolic rate, where  $E$  is the average activation energy of the respiratory complex ( $\approx 0.65$  eV;  $1 \text{ eV} = 1.602 \times 10^{-19}$  J), and  $k$  is the Boltzmann constant ( $8.62 \times 10^{-5}$  eV  $\text{K}^{-1}$ ). This Boltzmann–Arrhenius factor has been shown to describe the temperature dependence of metabolic rate for a broad assortment of organisms in recent work (12) and in much earlier work conducted near the beginning of the last century (18).

Recent work indicates that the generation time, expressed here as the individual turnover rate,  $g$  (generations  $\text{sec}^{-1}$ ), and the mutation rate,  $\alpha$  (mutations  $\cdot$  nucleotide $^{-1}\cdot\text{sec}^{-1}$ ), both show this same temperature dependence (12–14):

$$g = g_o \bar{B} = g_o B_o e^{-E/kT} \quad [2]$$

and

$$\alpha = \alpha_o \bar{B} = \alpha_o B_o e^{-E/kT}, \quad [3]$$

where  $g_o$  is the number of generations per joule of energy flux through a gram of tissue (generations  $\cdot \text{J}^{-1}\cdot\text{g}$ ), and  $\alpha_o$  is the number of mutations per nucleotide per joule of energy flux through a gram of tissue (mutations  $\cdot$  nucleotide $^{-1}\cdot\text{J}^{-1}\cdot\text{g}$ ). Eqs. 2 and 3 predict a 15-fold increase in the rates of individual turnover and mutation over the temperature range 0–30°C from the poles to the equator ( $e^{-E/k303}/e^{-E/k273} = 15$ -fold from 273–303 K). Because  $g$  and  $\alpha$  are both governed by  $\bar{B}$ , the number of mutations per nucleotide per generation,

$$\alpha_\tau = \alpha/g = \alpha_o/g_o \propto e^{0/kT}, \quad [4]$$

is independent of temperature.

Speciation entails genetic divergence among populations from a common ancestral lineage, resulting in reproductive isolation (2, 4). The theory of population genetics characterizes the rate of increase in the total genetic divergence,  $D$  (substitutions nucleotide $^{-1}$ ), between two reproductively isolated diploid pop-

Conflict of interest statement: No conflicts declared.

Freely available online through the PNAS open access option.

Abbreviations: CI, confidence interval; FO, first occurrence; Ma, mega-annum; SSU rDNA, small subunit rRNA-encoding DNA.

<sup>†</sup>To whom correspondence may be addressed. E-mail: drewa@nceas.ucsb.edu or jhbrown@unm.edu.

© 2006 by The National Academy of Sciences of the USA

ulations, both of size  $J_s$ , on a per-generation basis,  $dD/d\tau$  (substitutions·nucleotide<sup>-1</sup>·generation<sup>-1</sup>), such that

$$dD/d\tau = dD_0/d\tau + dD_+/d\tau \approx 2f_0\alpha_\tau + 8f_+J_s\alpha_\tau \approx 2f_0\alpha_\tau, \quad [5a]$$

where  $f_0$  and  $f_+$  are the respective fractions of mutations that are selectively neutral ( $s = 0$ ) and beneficial ( $s > 0$ ),  $D_0$  and  $D_+$  are the respective contributions of neutral and beneficial mutations to the total genetic divergence  $D$ , and

$$dD_0/d\tau = (4J_s f_0 \alpha_\tau) / (1/2J_s) = 2f_0\alpha_\tau \quad [5b]$$

and

$$dD_+/d\tau = (4J_s f_+ \alpha_\tau) \cdot ((1 - e^{-2s}) / (1 - e^{-4J_s s})) \approx 8f_+ J_s \alpha_\tau \quad [5c]$$

are the respective rates of fixation of neutral and beneficial mutations in the populations (3). Deleterious mutations ( $s < 0$ ) have only a negligible chance of fixation due to purifying selection (3) and are therefore excluded. Fixation rates increase with population size for beneficial mutations (Eq. 5c) but are independent of population size for neutral mutations (Eq. 5b). According to the neutral theory of molecular evolution (3), the overall rate of genetic divergence (Eq. 5a) should also be approximately independent of population size, because the number of neutral mutations far exceeds the number of beneficial ones, i.e.  $2f_0 \gg 8f_+ J_s$ . Gene flow among populations, characterized by the per-generation probability of individual migration (3), is not explicitly modeled. Eq. 5 therefore applies to allopatric speciation (19), which is widely regarded as the most common mode of speciation (4).

Combining Eqs. 1–4 from the metabolic theory with Eq. 5 from population genetics theory, we can derive an analytical model of speciation by making three simplifying assumptions. Assumption 1 is that the number of genetic changes required for reproductive isolation to evolve is independent of temperature. The genetic divergence between incipient taxa attributable to beneficial mutations,  $D_s^+$ , can serve as a proxy for this quantity, because empirical data indicate that the genes initially responsible for the evolution of reproductive isolation are generally under selection (4). Assumption 1 thus implies that  $D_s^+ \propto e^{0/kT}$ . Assumption 2 is that the population-level variables influencing genetic divergence rates are independent of temperature (i.e.,  $J_s \propto e^{0/kT}$  and  $s \propto e^{0/kT}$  in Eq. 5); these variables are governed by ecological details of the particular speciation mechanism facilitating genetic divergence (19). Together, Assumptions 1 and 2 predict that the time to speciation,  $t_s$  (sec), should decline exponentially with increasing temperature in the same way as the individual generation time,  $1/g$ ,

$$t_s = (1/g)(D_s^+)(d\tau/dD_+) \approx (1/g)(D_s^+)(1/8f_+J_s\alpha_\tau) \propto (1/g_0B_0)e^{E/kT}, \quad [6]$$

because the number of generations required for speciation to occur,  $t_s g \approx (D_s^+)(1/8f_+J_s\alpha_\tau)$  is independent of temperature when Assumptions 1 and 2 are upheld. Given that  $t_s g$  is independent of temperature and that the number of mutations per nucleotide per generation is also independent of temperature ( $\alpha_\tau$  in Eq. 4), the total genetic divergence between incipient species,  $D_s$  (substitutions nucleotide<sup>-1</sup>), should be independent of temperature as well:

$$D_s = (t_s g)(dD/d\tau) \approx (t_s g)(dD_0/d\tau) = (t_s g)(2f_0\alpha_\tau) \propto e^{0/kT}. \quad [7]$$

The germ-line replication rate is largely controlled by the individual turnover rate,  $g$ . Eqs. 6 and 7 therefore still apply if the genetic mechanism of speciation does not involve mutations of single nucleotides, which govern  $D_s^+$  and  $D_s$ , but instead involves some other form of mutation that occurs during germ-line replication, e.g., chromosomal transversions (4).

Assumption 3 is that, over global temperature gradients, time-averaged rates of genetic divergence are constrained by mutation rates and generation times of individuals, which govern speciation times for diverging populations ( $t_s$  in Eq. 6), and not by spatial gradients in the ecological mechanisms that facilitate genetic divergence. Ecological variables may, however, generate variation about the predicted temperature trends through their effects on population-level variables ( $J_s$  and  $s$  in Eq. 6). Assumption 3 implies that genetic divergence mechanisms are globally ubiquitous. This assumption is consistent with empirical observations that morphospecies of planktonic foraminifera are capable of global dispersal (20) yet comprise populations that exhibit significant levels of divergence among polar to tropical oceanic provinces (21–24). Together these two observations indicate that natural selection powerfully constrains effective rates of gene flow among foraminifera populations (25) and thereby facilitates genetic divergence among populations in relation to environmental gradients at all latitudes.

Assumptions 1–3 predict that the per capita speciation rate for an entire “metacommunity” of individuals involved in species-extinction dynamics (26),  $v$  (species·individual<sup>-1</sup>·sec<sup>-1</sup>), should scale inversely with the time to speciation,  $t_s$  (Eq. 6), and should therefore increase exponentially with temperature in the same way as individual metabolic rate,  $\bar{B}$  (Eq. 1),

$$v = v_0 e^{-E/kT} \propto (1/t_s) \propto \bar{B}, \quad [8]$$

where  $v_0$  is the speciation rate per individual per unit time (species·individual<sup>-1</sup>·sec<sup>-1</sup>). Expressing speciation on a per capita basis in Eq. 8 is consistent with Assumption 2 in that the sizes of genetically diverging populations,  $J_s$ , are independent of temperature and therefore independent of latitude. By expressing speciation on a per capita basis, we can use Eq. 8 to predict that the overall rate of speciation in the metacommunity,  $V_m$  (species sec<sup>-1</sup>), should increase linearly with total metacommunity abundance,  $J_m$ ,

$$V_m = J_m v = A_m J_A v_0 e^{-E/kT}, \quad [9]$$

and therefore with metacommunity area,  $A_m$  (km<sup>2</sup>), and with metacommunity abundance per unit area,  $J_A = J_m/A_m$ . These predictions follow directly from the model assumptions: Increases in  $J_m$  imply that greater numbers of size- $J_s$  populations are genetically diverging from each other at any given time and hence that  $V_m$  is higher.

## Results and Discussion

We begin by evaluating the predicted temperature dependence of mutation rates,  $\alpha$  (Eq. 3), by using a global compilation of small subunit ribosomal rRNA-encoding DNA (SSU rDNA) data obtained by sequencing nuclear genomes of planktonic foraminifera (see Appendix 1, which is published as supporting information on the PNAS web site). These data encompass evolutionary rates for 15 morphospecies whose geographic ranges collectively span arctic to tropical waters.

As predicted by Eqs. 3–5, the logarithm of the size-corrected rate of neutral molecular evolution,  $\ln(f_0\alpha M^{1/4})$ , is a linear function of ocean temperature,  $1/kT$  ( $r^2 = 0.34$ ;  $P = 0.003$ ; Fig. 1). Furthermore, the absolute value of the fitted slope yields a 95% confidence interval (CI) for  $E$  that closely matches the predicted value of 0.65 eV ( $\bar{x} = 0.67$  eV; 95% CI, 0.26–1.07 eV). Thus, after controlling for variation in foraminifera size, the

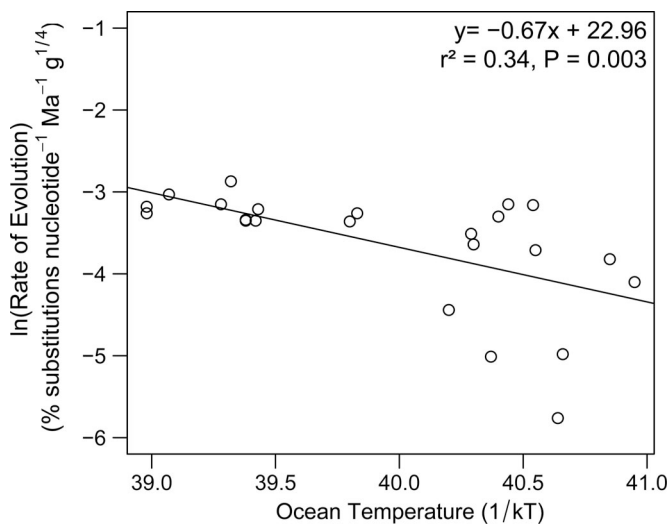


**Fig. 1.** Effect of ocean temperature,  $1/kT$ , on the size-corrected rate of neutral molecular evolution,  $\ln(f_o \alpha M^{1/4})$ , for nuclear genomes of planktonic foraminifera. The slope ( $-0.67$  eV) was fitted by using ordinary least-squares regression and is close to the value of  $-E \approx -0.65$  eV (95% CI,  $-0.26$  to  $-1.07$  eV), which was predicted based on the temperature dependence of individual metabolic rate (Eq. 3). Refer to Appendix 1 for details on this global compilation of SSU rDNA data.

temperature-dependence of nuclear DNA evolution matches the prediction derived in Eq. 3 based on the activation energy of individual metabolic rate. Importantly, we derive this relationship by characterizing habitat temperatures by using sea-surface temperature data for shallow-dwelling taxa and temperatures at 200-m depth for deeper-dwelling taxa (see Appendix 1). If, instead, we characterize habitat temperatures by using sea-surface temperature data for all taxa, the slope of the relationship between  $\ln(f_o \alpha M^{1/4})$  and  $1/kT$  still yields a 95% CI for  $E$  that includes the predicted value of  $0.65$  eV ( $0.04$ – $1.45$  eV), but the correlation is weaker ( $r^2 = 0.18$  versus  $0.34$  for the model in Fig. 1). This finding supports the hypothesis that deeper-dwelling taxa exhibit lower size-corrected rates of molecular evolution as a direct consequence of declines in habitat temperature with increasing depth. Thus, it appears that thermal habitat preference significantly influences rates of DNA evolution for this group.

The results in Fig. 1 represent previously unrecognized and direct evidence, based on well established fossil calibrations (see Appendix 1), that absolute rates of DNA evolution increase exponentially with environmental temperature in the same way as individual metabolic rate. These results also serve to reinforce and extend previous work indicating that absolute rates of mitochondrial DNA evolution are higher for warmer-bodied endotherms than for ectothermic animals of similar size (14, 16) and that relative rates of nuclear DNA evolution increase with environmental temperature for plants (27–29). Note that our model predicts that rates of molecular evolution should increase exponentially with environmental temperature for ectotherms but not for endotherms, which maintain body temperatures of  $\approx 35$ – $40^\circ\text{C}$  during active periods, regardless of ambient temperature. Hence, our model and results do not contradict a study of birds, which found “no support for an effect of latitude on rate of molecular evolution” (30).

We evaluate the predicted temperature dependence for the genetic divergence between incipient species,  $D_s$  in Eq. 7, by using a global compilation of SSU rDNA data for  $>20$  “cryptic” taxa (23) that have been identified within seven morphospecies of planktonic foraminifera (see Appendix 2, which is published

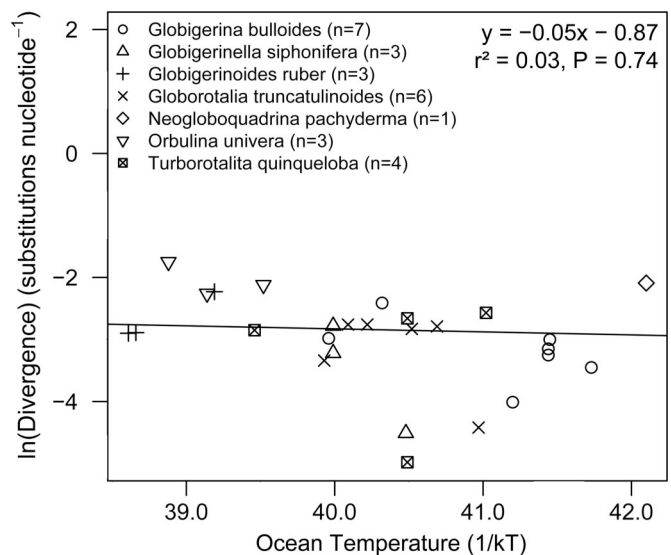


**Fig. 2.** Effect of ocean temperature,  $1/kT$ , on genetic divergence,  $\ln(D_s)$ , for nuclear genomes of ecologically distinct genotypes within seven morphospecies of planktonic foraminifera. The sample sizes in the legend refer to the numbers of pairwise comparisons among populations comprising each morphospecies. The data were weighted such that each morphospecies contributed equally to the ordinary least-squares regression slope, which does not differ from the predicted value of 0 (Eq. 7). This conclusion remains unchanged if data points, rather than morphospecies, are weighted equally ( $P = 0.10$ ). Refer to Appendix 2 for details on this global compilation of SSU rDNA data.

as supporting information on the PNAS web site). These cryptic taxa are ecologically distinct genotypes with different geographic distributions (21–24, 31) and temperature optima (23). They are therefore thought to represent incipient morphotaxa in the relatively early stages of speciation (24).

Despite evidence indicating that rates of molecular evolution increase exponentially with environmental temperature (Fig. 1), the genetic divergence between incipient taxa is independent of ocean temperature (Fig. 2;  $P = 0.74$ ), as predicted by Eq. 7. These findings are consistent with Assumptions 1 and 2 of our model that  $D_s^+$ ,  $J_s$ , and  $s$  are all independent of temperature. We note, however, that the data depicted in Fig. 2 encompass taxon pairs at various stages of divergence, not just the incipient stage, which is fleeting and therefore difficult to observe (4).

We evaluate latitudinal gradients in rates of speciation at the level of metacommunities,  $V_m$  (Eq. 9), by using fossil data compiled in the Neptune database, which span the last 30 million years (Ma) of macroevolution for planktonic foraminifera (32). Our analysis involves assessing how the rate of first occurrence (FO) of new morphospecies, which is a surrogate measure for the speciation rate (10), varies across latitudes at the global scale. When analyzing and interpreting these data, it is important to recognize that each morphospecies may evolve to comprise several distinct genotypes that occupy different thermal environments, as shown in Fig. 2.

By using these fossil data, we show that the time-averaged rate of speciation is significantly higher in the tropics (Fig. 3A, equal-area latitudinal bands 2 and 3) than in the temperate zones (Fig. 3A, bands 1 and 4), even after controlling for sampling effort and for the greater habitat area at tropical latitudes (Fig. 3B; and see Appendix 3, which is published as supporting information on the PNAS web site). Furthermore, this gradient in macroevolutionary dynamics is significantly correlated with average ocean temperatures ( $r^2 = 0.97$ ;  $P = 0.01$ ; Fig. 3B), which have been estimated by using a robust paleotemperature calibration (33) to control for the  $\approx 8^\circ\text{C}$  decline in high-latitude ocean temperatures

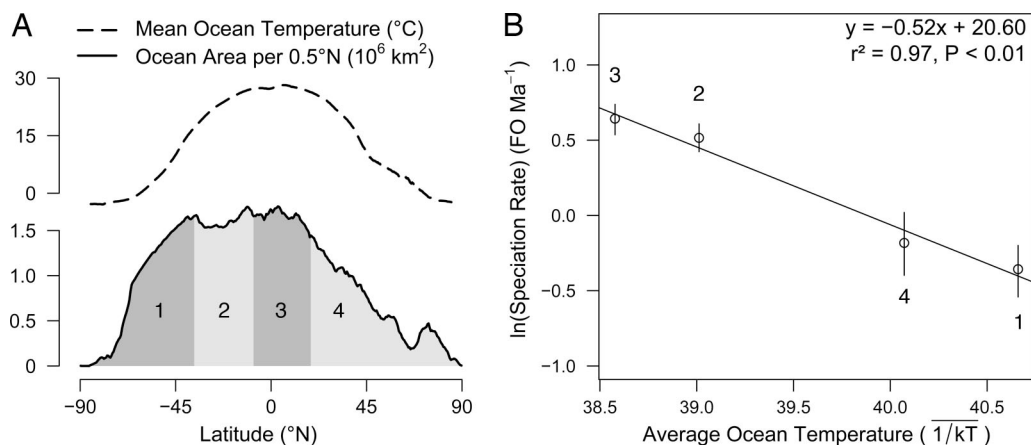


**Fig. 3.** Both ecological and macroevolutionary variables exhibit pronounced variation from the poles to the equator. (A) Depicted are the latitudinal gradient in contemporary mean annual sea-surface temperatures (48) (dashed line) and ocean surface area per 0.5° latitude (solid line; negative numbers correspond to southern latitudes). Different shades are used to represent four equal-area latitudinal bands of  $\approx 9.1 \times 10^7$  km<sup>2</sup> ocean area each. (B) Depicted are the effects of ocean temperature on time-averaged speciation rates over the past 30 Ma in each of the four equal-area latitudinal bands. The line was fitted by using ordinary least-squares regression. Speciation rates were calculated based on the latitudinal distribution of >150 FO of foraminifera morphospecies by using the Neptune database (32); 95% CIs (vertical lines) were generated, as described in Appendix 3, by using a randomization procedure that explicitly controls for the effects of variation in sampling efforts on paleontological analyses. The average sea-surface temperature within each latitudinal band over the past 30 Ma was estimated, as described in Appendix 4, by using a robust paleotemperature calibration (33).

over the past 30 Ma (see Appendix 4, which is published as supporting information on the PNAS web site). According to our model, this correlation reflects the combined effects of temperature-dependent changes in the per capita speciation rate,  $\nu$  (Eq. 8), and in total community abundance per unit area,  $J_A$  (Eq. 9), because only ocean area,  $A_m$ , is held constant for the metacommunity-level rates depicted in Fig. 3B.

Importantly, the strength of this correlation may be sensitive to the number and placement of latitudinal bands, because FO events for ocean plankton are unevenly distributed across latitudes, as shown in another study conducted with the Neptune database (32). These findings are consistent with the hypothesis that speciation events for marine taxa are often concentrated along the margins of oceanographic currents, because these currents facilitate divergent selection, genetic divergence, and speciation (34, 35). In our model, oceanographic currents could enhance speciation rates through their effects on population subdivision ( $J_s$ ), the intensity of natural selection ( $s$ ), and/or metacommunity abundance ( $J_A$ ) (Eqs. 5–9).

To control for any effects of spatial aggregation of FO events on the estimated rates of macroevolution, we evaluate the predicted temperature dependence of the per capita speciation rate,  $\nu$  (Eq. 8), by using an alternative approach that explicitly controls for latitudinal covariation in ocean area, temperature, and metacommunity abundance per unit area,  $J_A$  (Eq. 9), without having to bin the FO data into arbitrary regions (Appendix 5, which is published as supporting information on the PNAS web site). By using this alternative approach, we obtain a 95% CI for  $E$  that includes the predicted value of 0.65 eV ( $\bar{x} = 0.78$  eV; 95% CI, 0.62–0.96 eV). Thus, after controlling for variation in foraminifera community abundance across latitudes, the temperature-dependence of speciation matches the prediction derived in Eq. 8 based on the activation energy of individual metabolic rate. These results support Assumption 3 of our model that variation in speciation rates across global temperature gradients is largely controlled by the same individual-level variables constraining rates of genetic divergence among populations (i.e., generation times and mutation rates in Eqs. 2 and 3).

The model and results presented here yield four insights into the factors governing the origin and maintenance of biodiversity.

The first insight is that energy flux is a primary determinant of evolutionary dynamics. Consequently, the rates of nucleotide substitution (Fig. 1) and per capita speciation both vary exponentially with temperature according to the same Boltzmann–Arrhenius factor controlling individual metabolic rate ( $e^{-E/kT}$  in Eq. 1). The second insight is that the total genetic change required to produce a new species, characterized by  $D_s$ , is independent of temperature (Fig. 2) and therefore independent of latitude and metabolic rate. Our model and results support the hypothesis that the tropics are a “cradle” for biodiversity (10, 36), because a given amount of genetic change results in the same degree of ecological and morphological differentiation, regardless of the temperature regime, but takes exponentially less time in a hotter environment (Eq. 6) due to shorter generation times (Eq. 2) and higher mutation rates (Eq. 3). Consequently, “effective” evolutionary time per unit absolute time is greater at tropical latitudes, as proposed by Rohde (37).

The third insight is that a fixed quantity of energy is required, on average, to produce a given magnitude of evolutionary change. We showed earlier that  $\approx 2.5 \times 10^{13}$  J of energy must be fluxed per gram of tissue to induce one substitution per nucleotide in nuclear genomes of primates (14). That estimate is remarkably close to the value determined here of  $\approx 1.8 \times 10^{13}$  J g<sup>-1</sup> for nuclear genomes of foraminifera (see *Methods*). Similarly, a fixed but much larger quantity of energy must be fluxed through a population to produce a new morphospecies of foraminifera, independent of environmental temperature and hence latitude. We estimate this quantity to be  $b_o \bar{M}^{3/4} / \nu_o \approx 10^{23}$  J based on estimates for  $b_o \approx 2.8 \times 10^7$  W g<sup>-3/4</sup> (17),  $\nu_o \approx 5.6 \times 10^{-20}$  species·individual<sup>-1</sup>·sec<sup>-1</sup> (see Appendix 5), and the geometric mean of the foraminifera mass estimates in Appendix 1,  $\bar{M} \approx 5.7 \times 10^{-5}$  g. This is an enormous quantity of energy; it exceeds global net primary production for an entire year ( $\approx 10^{21}$  J) (38) and current annual fossil fuel consumption by all of humanity ( $\approx 10^{20}$  J) (39). We expect this quantity to vary with the mode of speciation and hence with taxon and environmental setting, because the absolute rate of genetic divergence is a function not only of individual-level variables governed by metabolic rate (i.e., generation times and mutation rates) but also of gene flow, effective population size, and the intensity of natural selection. This example highlights the need to better understand how individual-level variables (Eqs. 2 and 3) combine with spatially explicit

population-level processes to determine the temperature-dependence of speciation rates (Eq. 8).

The fourth insight is that habitat area is also an important determinant of latitudinal gradients in speciation rates and hence biodiversity, as suggested by Rosenzweig (6). In fact, our model and results indicate that the predicted exponential effects of temperature on speciation rates are only manifested after controlling for habitat area and community abundance by expressing speciation on a per capita basis (Eq. 8). This approach runs counter to the long-standing tradition among evolutionary biologists and paleontologists of expressing speciation on a per species basis ( $\text{species} \cdot \text{species}^{-1} \cdot \text{time}^{-1}$ ) (4). Nevertheless, it is consistent with evolutionary theory, because speciation occurs at the level of populations (Eqs. 5–9). It is also consistent with the recently proposed neutral biodiversity theory (NBT) of Hubbell (26), which predicts that the per capita speciation rate,  $\nu$ , determines the number of species maintained in a metacommunity of fixed abundance  $J_m$ . Synthesizing our energetically and genetically based model of speciation (Eqs. 1–9) with NBT may therefore yield a better understanding of why biodiversity increases exponentially with environmental temperature in the same way as individual metabolic rate for diverse groups of terrestrial, aquatic, and marine ectotherms (7, 40, 41).

We conclude by noting that the theory developed here also predicts that evolutionary rates vary as a power function with body size according to the mass-dependence of individual metabolic rate ( $\propto M^{-1/4}$ ). This result has been shown for rates of microevolution, i.e., nucleotide substitution (14), but has not yet been demonstrated for rates of macroevolution. Extension of our model may therefore yield insights into the combined effects of body size and temperature on other prominent yet poorly understood gradients in macroevolutionary dynamics (for examples, see refs. 42 and 43).

## Methods

**Molecular Evolution Data.** The SSU rDNA data in Fig. 1 were compiled from the sources cited in Appendix 1. Our model predicts that rates of molecular evolution increase exponentially with temperature (Eq. 3), which implies that the warmer, more rapidly evolving taxon makes a greater contribution to the genetic divergence,  $D$ , and hence to the calculated rate of molecular evolution  $f_o\alpha = D/2\Gamma$  (following Eq. 5), where  $\Gamma$  is the time since divergence. To account for the greater contribution of the warmer-bodied taxon to  $f_o\alpha$ , we characterize the overall habitat temperature for each taxon pair depicted in Fig. 1 by using the Boltzmann average,

$$\langle T \rangle_E = -E / \ln((e^{-E/kT_1} + e^{-E/kT_2}) / 2)k,$$

where  $T_1$  and  $T_2$  are the habitat temperatures of the two taxa in Kelvins. Habitat temperatures were independently estimated by using a global compilation of contemporary community abundance data collected from 1,265 sites around the world (44) in conjunction with contemporary ocean temperature data (45). Habitat temperatures were estimated by using sea-surface temperatures for shallow-dwelling taxa and temperatures at 200-m depth for deeper-dwelling taxa (Appendix 1).

**Genetic Divergence Data.** The SSU rDNA data in Fig. 2 were compiled from the sources cited in Appendix 2. The habitat temperature of each population was estimated from the spatial location of sampling by using contemporary ocean temperature data (45). The Boltzmann-averaged habitat temperature,  $\langle T \rangle_E$ , was then calculated for each taxon pair depicted in the figure.

**FO Data.** The latitudinal distribution of FOs of morphospecies in Fig. 3B was analyzed by using morphospecies-level data in the Neptune database, a compilation of fossil samples from over 160 deep-sea drilling holes around the world that have been dated to an average precision of  $<1$  Ma (32). We analyzed the Neptune data by using the following procedure to simultaneously control for latitudinal variation in area (Fig. 3A) and for the effects of sampling effort on paleontological analyses (46): (i) We assigned each of  $>3,000$  core samples to one of four latitudinal bands of equal ocean surface area (Fig. 3A) and to one of six 5-Ma time intervals spanning the last 30 Ma. (ii) We selected a subset of 40 samples at random and without replacement from each equal-area latitudinal band and time interval, yielding a data subset comprising  $>900$  samples. (iii) We determined the band of FO for each morphospecies of foraminifera arising through speciation over the past 30 Ma. (iv) We tallied the total number of FOs in each band to obtain estimates for  $V_m$ . (v) We repeated steps ii–iv 100 times to generate the 95% CIs for  $V_m$  depicted in Fig. 3B (Appendix 3).

**Paleotemperature Data.** To obtain the estimates of average ocean temperature depicted in Fig. 3B,  $1/kT$ , we modeled variation in sea-surface temperatures with respect to latitude,  $L$  ( $-90^\circ$  to  $90^\circ$ N), and time,  $t$ , by using the heat equation on the surface of a sphere,  $T(L, t) = (P(t) - T_0)\sin^2(\pi L/180) + T_0$ , where  $P(t)$  is the sea-surface temperature at the poles at time  $t$ , and  $T_0$  is the sea-surface temperature at the equator. The function  $P(t)$  was estimated in Fig. 2 of ref. 33 by using robust methods of paleotemperature calibration. The parameter  $T_0$  was assumed to remain constant at  $\approx 28^\circ\text{C}$  over the past 30 Ma based on available evidence (47). The function  $T(L, t)$  was integrated over time and space, as described in Appendix 4, to yield the estimates of  $1/kT$  depicted in Fig. 3B.

**Estimating the per Capita Speciation Rate.** Evaluating the temperature dependence of the per capita speciation rate (Eq. 8) required explicitly accounting for temperature-dependent changes in foraminifera community abundance across latitudes. To avoid difficulties associated with inferring live abundances of foraminifera from shell accumulation rates, we characterized this temperature dependence by using a global compilation of plankton tow data (45) on foraminifer metacommunity abundance per unit area,  $J_A$ . We estimated the temperature dependence of the per capita speciation rate, characterized by  $E$  (Eq. 8), and the normalization parameter,  $\nu_o$ , by expressing the latitudinal distribution of FOs as a cumulative function of ocean area (Fig. 3A), paleotemperature  $T(L, t)$ , and metacommunity abundance (Appendix 5).

**Estimating the Energy Required to Induce Mutations.** Following Eqs. 2–5, the size- and temperature-corrected rate of molecular evolution,  $f_o\alpha M^{1/4} e^{E/kT}$ , is equal to  $f_o\alpha_o b_o$ . For primates, we obtain an estimate of  $2.5 \times 10^{13} \text{ J} \cdot \text{g}^{-1} \cdot \text{substitutions}^{-1} \cdot \text{nucleotide}$  for  $1/f_o\alpha_o$  by using an estimate of  $b_o \approx 3.9 \times 10^8 \text{ W} \cdot \text{g}^{-3/4}$  for endotherms (17) and the geometric mean of the estimates of  $f_o\alpha M^{1/4} e^{E/kT}$  in ref. 14 for the globin gene ( $\approx 4.9 \times 10^{10} \text{ substitutions} \cdot \text{nucleotide}^{-1} \cdot 10^{-8} \text{ yr} \cdot \text{g}^{1/4}$ ). For planktonic foraminifera, we obtain an estimate of  $1.8 \times 10^{13} \text{ J} \cdot \text{g}^{-1} \cdot \text{substitutions}^{-1} \cdot \text{nucleotide}$  for  $1/f_o\alpha_o$  by using an estimate of  $b_o \approx 2.8 \times 10^7 \text{ W} \cdot \text{g}^{-3/4}$  for unicells (17) and the geometric mean of the estimates of  $f_o\alpha M^{1/4} e^{E/kT}$  for the data depicted in Fig. 1 ( $\approx 5.0 \times 10^9 \text{ substitutions} \cdot \text{nucleotide}^{-1} \cdot 10^{-8} \text{ yr} \cdot \text{g}^{1/4}$ ).

We thank Fangliang He, Andrew Martin, Richard Norris, Klaus Rohde, and John Wilkins for their insightful comments and suggestions. A.P.A. was supported as a Postdoctoral Associate at the National Center for Ecological Analysis and Synthesis, a center funded by National Science Foundation Grant DEB-0072909, and the University of California, Santa Barbara. V.M.S. was supported by National Institutes of Health Grant 1 P50 GM68763-02 through the Bauer Center for Genomics Research.

1. Simpson, G. G. (1944) *Tempo and Mode in Evolution* (Oxford Univ. Press, London).
2. Dobzhansky, T. (1937) *Genetics and the Origin of Species* (Columbia Univ. Press, New York).
3. Kimura, M. (1983) *The Neutral Theory of Molecular Evolution* (Cambridge Univ. Press, Cambridge, U.K.).
4. Coyne, J. A. & Orr, H. A. (2004) *Speciation* (Sinauer, Sunderland, MA).
5. Rohde, K. (1992) *Oikos* **65**, 514–527.
6. Rosenzweig, M. L. (1995) *Species Diversity in Space and Time* (Cambridge Univ. Press, Cambridge, U.K.).
7. Allen, A. P., Brown, J. H. & Gillooly, J. F. (2002) *Science* **297**, 1545–1548.
8. Stehli, F. G., Douglas, D. G. & Newell, N. D. (1969) *Science* **164**, 947–949.
9. Crane, P. R. & Lidgard, S. (1989) *Science* **246**, 675–678.
10. Jablonski, D. (1993) *Nature* **364**, 142–144.
11. Brown, J. H., Gillooly, J. F., Allen, A. P., Savage, V. M. & West, G. B. (2004) *Ecology* **85**, 1771–1789.
12. Gillooly, J. F., Brown, J. H., West, G. B., Savage, V. M. & Charnov, E. L. (2001) *Science* **293**, 2248–2251.
13. Savage, V. M., Gillooly, J. F., Brown, J. H., West, G. B. & Charnov, E. L. (2004) *Am. Nat.* **163**, E429–E441.
14. Gillooly, J. F., Allen, A. P., West, G. B. & Brown, J. H. (2005) *Proc. Natl. Acad. Sci. USA* **102**, 140–145.
15. Shigenaga, M. K., Gimeno, C. J. & Ames, B. N. (1989) *Proc. Natl. Acad. Sci. USA* **86**, 9697–9701.
16. Martin, A. P. & Palumbi, S. R. (1993) *Proc. Natl. Acad. Sci. USA* **90**, 4087–4091.
17. Gillooly, J. F., Allen, A. P., Brown, J. H., Elser, J. J., Martinez del Rio, C., Savage, V. M., West, G. B., Woodruff, W. H. & Woods, H. A. (2005) *Proc. Natl. Acad. Sci. USA* **102**, 11923–11927.
18. Krogh, A. (1916) *Respiratory Exchange of Animals and Man* (Longmans Green, London).
19. Gavrillets, S. (2003) *Evolution (Lawrence, Kans.)* **57**, 2197–2215.
20. Darling, K. F., Wade, C. M., Stewart, I. A., Kroon, D., Dingle, R. & Brown, A. J. L. (2000) *Nature* **405**, 43–47.
21. de Vargas, C., Norris, R., Zaninetti, L., Gibb, S. W. & Pawlowski, J. (1999) *Proc. Natl. Acad. Sci. USA* **96**, 2864–2868.
22. Darling, K. F., Wade, C. M., Kroon, D., Brown, A. J. L. & Bijma, J. (1999) *Paleoceanography* **14**, 3–12.
23. Kucera, M. & Darling, K. F. (2002) *Philos. Trans. R. Soc. London A* **360**, 695–718.
24. Darling, K. F., Kucera, M., Pudsey, C. J. & Wade, C. M. (2004) *Proc. Natl. Acad. Sci. USA* **101**, 7657–7662.
25. Endler, J. A. (1977) *Geographic Variation, Speciation, and Clines* (Princeton Univ. Press, Princeton).
26. Hubbell, S. P. (2001) *A Unified Neutral Theory of Biodiversity and Biogeography* (Princeton Univ. Press, Princeton).
27. Wright, S. D., Gray, R. D. & Gardner, R. C. (2003) *Evolution (Lawrence, Kans.)* **57**, 2893–2898.
28. Davies, T. J., Savolainen, V., Chase, M. W., Moat, J. & Barraclough, T. G. (2004) *Proc. R. Soc. London Ser. B* **271**, 2195–2200.
29. Wright, S., Keeling, J. & Gillman, L. (2006) *Proc. Natl. Acad. Sci. USA* **103**, 7718–7722.
30. Bromham, L. & Cardillo, M. (2003) *J. Evol. Biol.* **16**, 200–207.
31. Huber, B. T., Bijma, J. & Darling, K. (1997) *Paleobiology* **23**, 33–62.
32. Spencer-Cervato, C. (1999) *Palaeontologia Electronica* **2** (2), article 4.
33. Zachos, J., Pagani, M., Sloan, L., Thomas, E. & Billups, K. (2001) *Science* **292**, 686–693.
34. Palumbi, S. R. (1994) *Annu. Rev. Ecol. Syst.* **25**, 547–572.
35. Norris, R. D. (2000) *Paleobiology* **26**, 236–258.
36. Stenseth, N. C. (1984) *Oikos* **43**, 417–420.
37. Rohde, K. (1978) *Biol. Zent. Bl.* **97**, 393–403.
38. Field, C. B., Behrenfeld, M. J., Randerson, J. T. & Falkowski, P. (1998) *Science* **281**, 237–240.
39. Dukes, J. S. (2003) *Clim. Change* **61**, 31–44.
40. Kaspari, M., Ward, P. S. & Yuan, M. (2004) *Oecologia* **140**, 407–413.
41. Hunt, G., Cronin, T. M. & Roy, K. (2005) *Ecol. Lett.* **8**, 739–747.
42. Norris, R. D. (1991) *Paleobiology* **17**, 388–399.
43. Alroy, J. (1998) *Science* **280**, 731–734.
44. Prell, W., Martin, A., Cullen, J. & Trend, M. (1999) *The Brown University Foraminiferal Database* (National Oceanic & Atmospheric Administration/National Geophysical Data Center Paleoclimatology Program, Boulder CO).
45. Conkright, M. E., Antonov, J. I., Baranova, O., Boyer, T. P., Garcia, H. E., Gelfeld, R., Johnson, D., Locarnini, R. A., Murphy, P. P., O'Brien, T. D., et al. (2002) *World Ocean Database* (U.S. Government Printing Office, Washington, DC), Vol. 1.
46. Alroy, J., Marshall, C. R., Bambach, R. K., Bezusko, K., Foote, M., Fursich, F. T., Hansen, T. A., Holland, S. M., Ivany, L. C., Jablonski, D., et al. (2001) *Proc. Natl. Acad. Sci. USA* **98**, 6261–6266.
47. Crowley, T. J. & Zachos, J. C. (2000) in *Warm Climates in Earth History* (Cambridge Univ. Press, New York), pp. 50–76.
48. Casey, K. S. & Cornillon, P. (1999) *J. Climate* **12**, 1848–1863.